

A Novel Low Profile Polarization Insensitive Electromagnetic Shield for X-Band Applications

Muhammad Idrees
College of Electronics and Information
Engineering, Shenzhen University,
Shenzhen, China
✉ muidrees169@gmail.com

Sai-Wai Wong
College of Electronics and Information
Engineering, Shenzhen University,
Shenzhen, China
wsw@szu.edu.cn

Yejun He
College of Electronics and Information
Engineering, Shenzhen University,
Shenzhen, China
heyejun@126.com

Saifullah Khalid
National University of Sciences and
Technology (NUST), Islamabad,
Pakistan
sukhalid@gmail.com

Muhammad Ali Khalid
Design and Development Cell, R&D
National Radio and Telecommunication
Corporation (NRTC), Haripur, Pakistan
10mseemkhalid@seecs.edu.pk

Muhammad Zeeshan Sarwar
Department of Telecom. Engineering
University of Engineering and
Technology (UET) Taxila, Pakistan
zeeshan.sarwar@uettaxila.edu.pk

Abstract—In this paper, a novel polarization-insensitive frequency-selective surface-based electromagnetic shield is presented for EMI shielding applications. The FSS unit cell consists of a modified Jerusalem crossed loop designed over a low-loss substrate. It achieves an effective shielding at 10 GHz frequency in the X-band. Moreover, it manifests a fractional bandwidth of 24%. In addition, the FSS offers angularly stable response up to 60 degrees for both TE and TM polarizations due to its symmetrical structure. The overall unit cell dimensions are $5.25 \times 5.25 \text{ mm}^2$. Thus, the proposed design is a promising candidate for narrowband SATCOM applications.

Keywords— Frequency Selective Surface, Polarization Insensitive, Electromagnetic Interference (EMI), Spatial Filter, stopband, Electromagnetic compatibility.

I. INTRODUCTION

Frequency selective surfaces (FSSs) are the periodic arrangements of metallic elements in two or three dimensions that show a band-stop or bandpass filtering response when illuminated with electromagnetic waves. FSSs, due to their widespread applications, find their employability in antenna radome design, RCS reduction, analog absorbers, artificial magnetic conductors (AMCs), EBG structures, performance enhancement of antennas, antenna reflectors, High Impedance Surfaces, electromagnetic interference mitigation, satellite communication services, and many others [1-6].

Many FSS configurations are recently reported for various applications. In [6], a single layer polarization-insensitive FSS is studied for EM shielding in the C-band. A corner modified square-ring FSS in [7] shows a polarization-insensitive ultra-wideband response with an attenuation of 47.8 dB. A crossed dumbbell-shaped in [8] and annual ring and flower-shaped FSS in [9], are reported to suppress Wi-Fi and WLAN signals. Another single layer FSS with dual stopband functionality in [10] is proposed for X-band shielding. In addition, in [11], a U-shaped FSS provides shielding in the X and Ku bands. In [12], a dual-band modified square loop FSS is presented for GSM shielding applications. A meander-line FSS geometry in [13] offers RF-shielding for building.

In this paper, a novel miniaturized FSS based EM shield is presented. The FSS consists of a modified Jerusalem cross loop which offers 45 dB attenuation at the desired frequency. In addition, it shows good angular stability up to 60° for both TE and TM mode polarization. Rest of the paper is organized as sections II and III describe unit cell design-process, results, and discussions. Finally, section IV concludes the paper.

II. UNIT CELL DESIGN CONFIGURATION

The unit cell of the proposed FSS is shown in Figure 1. The FSS is designed on a low loss Rogers 5880 slab having thickness $t = 0.787 \text{ mm}$, $\epsilon_r = 2.2$ and $\tan\delta = 0.0009$. Thus, the unit cell has compact dimensions of $5.25 \times 5.25 \text{ mm}^2$.

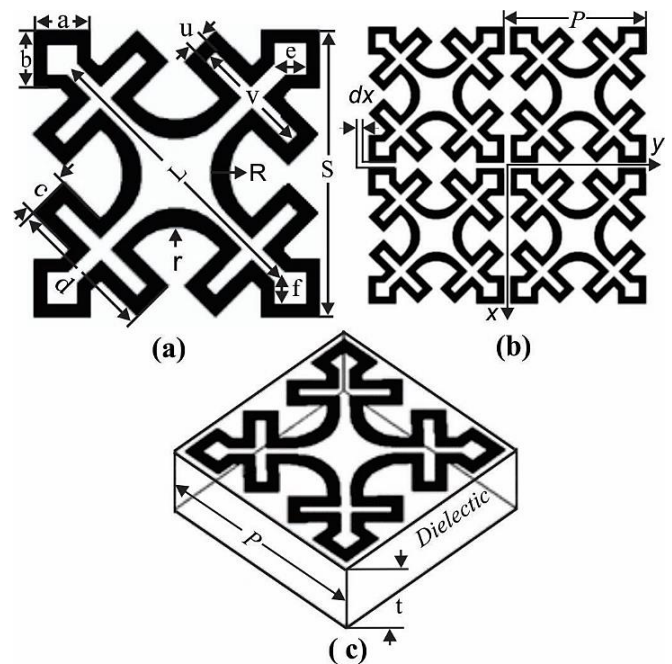


Figure 1: Proposed FSS Unit Cell top view, 2x2 array, and 3D view

The geometry of the proposed FSS is principally evolved through a four-step procedure, as shown in Fig. 2. The FSS consists of a crossed dipole of length 'L' placed diagonally on one side of the laminate, as shown in Fig. 2a. A rectangular strip is etched from the middle to make a crossed dipole loop to achieve miniaturization in structure. In addition, a square loop is incorporated at each leg of the crossed dipole loop to get desired response and to miniaturize the unit cell further, as illustrated in Fig. 2b. Moreover, Fig. 2c shows that a rectangular loop is joined with the geometry to increase its electrical length and achieve maximum attenuation at the frequency of interest. The resulting structure resembles a Jerusalem crossed loop shape. Furthermore, the edges at the center of the structure are chamfered at radii of 'r' and 'R'. These radii are optimized to achieve stopband in the X-band centered at 10 GHz frequency. Table I shows optimized values of design parameters, and all units are in mm.

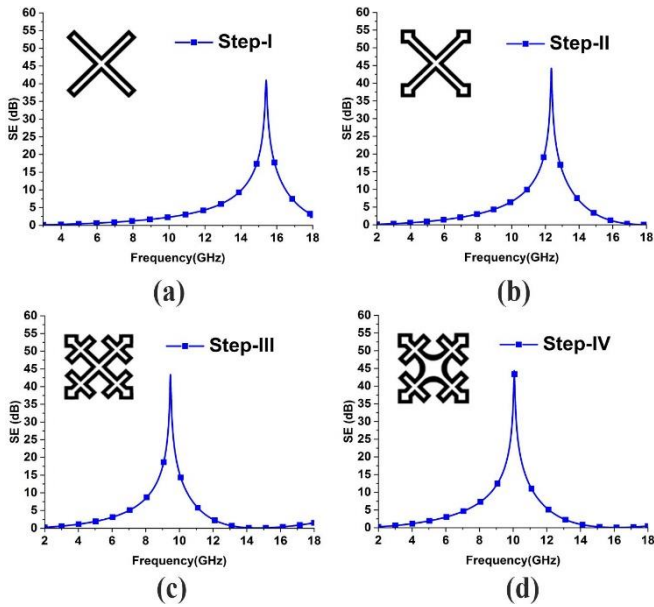


Figure 2: Design process of proposed FSS structure

III. RESULTS AND DISCUSSIONS

A. Electromagnetic Shielding Analysis

The proposed structure is designed and simulated in Ansys HFSS. The performance of the FSS is analyzed in terms of shielding effectiveness which can be expressed as in eq (1). The FSS achieves an effective shielding of at least 45 dB centered at 10 GHz frequency. The FSS has been further examined for various incidence angles as well as polarization states. Figure 3 shows the SE of the FSS unit cell as a function of frequency. It is observed that the unit cell shows an identical response for both the parallel and perpendicular polarization states of the incident wave at normal incidence owing to its four-fold symmetric geometry.

$$SE(dB) = -20 \times \log_{10} \left| \frac{E_t}{E_i} \right| \quad (1)$$

B. Angular Stability

The angular response of the FSS for TE and TM wave modes is illustrated in Figs. 4 and 5, correspondingly. The results show that the FSS offers good angular stability towards angle variations. It is observed that the FSS shows an almost identical response for both TE and TM polarizations when the oblique incident angle is varied from 0 to 60°. However, a grating lobe occurs at higher frequencies when the oblique angle is 30° and 60°. This second resonance is shifted upward as the incident angle increases and notch selectivity is improved. Moreover, the FSS offers a fractional bandwidth of 24% at normal incidence, which slightly increases within the acceptable limits as the incident angle varies. Table II shows fractional bandwidth variations as a function of oblique angle variations. Thus, the FSS manifests narrow bandwidth, which makes it suitable for narrowband operations. In addition, attenuation and selectivity are also improved as the angle is increased. Additionally, a 2×2 array response for TE and TM wave modes at normal incidence is illustrated in Fig. 6. It may be observed that the array has a similar response as the single unit cell. Correspondingly, the performance is alike over oblique angle variations as well.

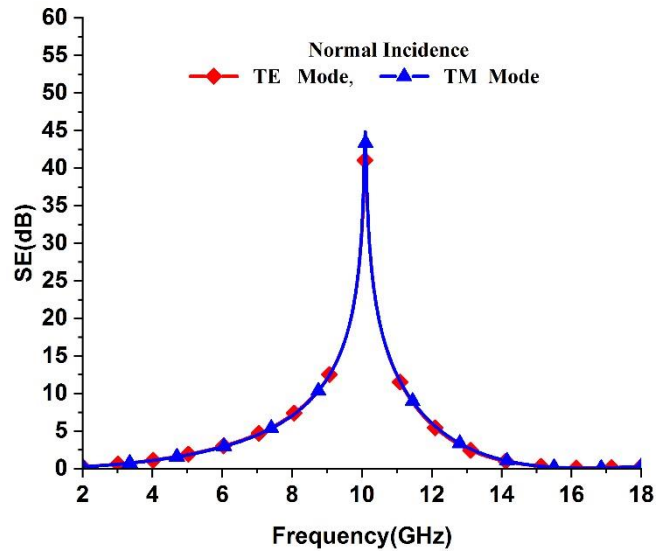


Figure 3: SE at normal incidence for TE and TM polarizations

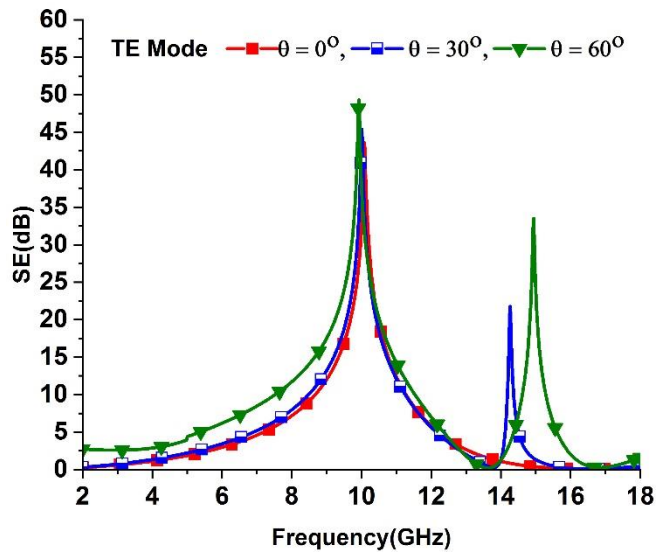


Figure 4: SE as a function of oblique incident angle for TE wave mode

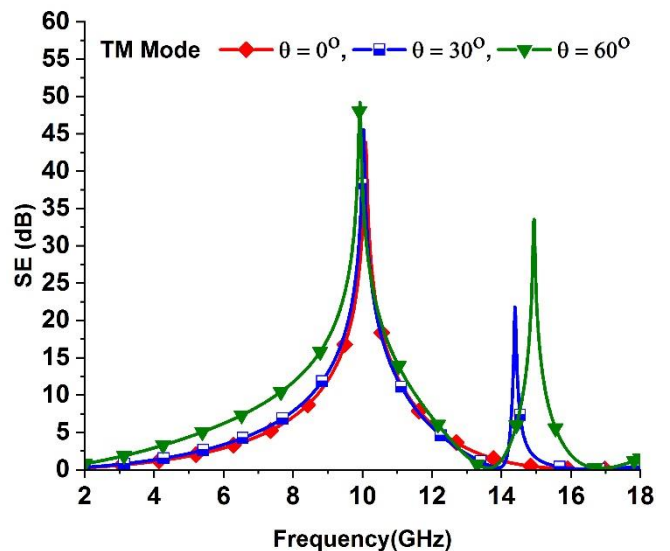


Figure 5: SE as a function of oblique incident angle for TM polarization mode

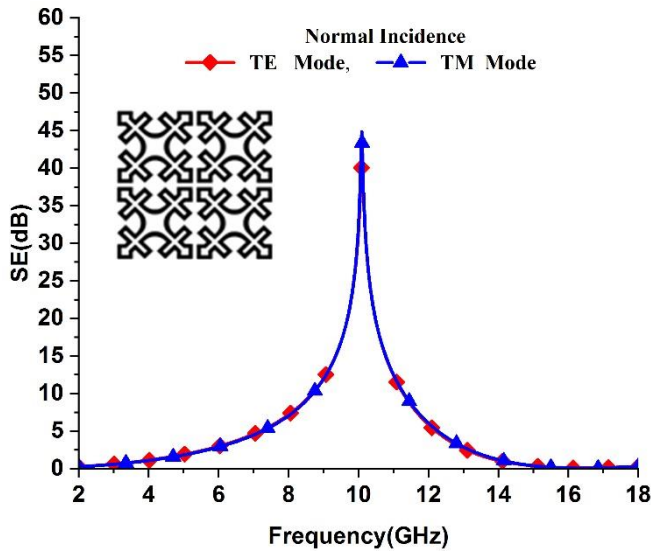


Figure 6: A 2x2 array response at normal incidence

TABLE I. OPTIMIZED DIMENSIONS OF FSS UNIT CELL AND ARRAY

Parameter	Value	Parameter	Value	Parameter	Value
r	1	d	2.5	S	5
R	0.9	e=f	0.5	P	5.25
a=b	1	u	0.25	Dx = Dy	0.35
c	0.75	v	2	t	0.787

TABLE II. FRACTIONAL BANDWIDTH AS A FUNCTION OF INCIDENCE ANGLE

Angle (θ)	Attenuation dB	TE-mode (%)	TE-mode (%)
0°	45.8/46.3	24.17	26.06
30°	46.5/46.7	28.05	27.70
60°	50.1/52.0	42.05	42.04

C. Parametric Analysis

The SE of FSS is analyzed in terms of the relative permittivity of the laminate. Figure 7 shows SE as a function of dielectric permittivity. It is observed that the SE curves slightly shifts towards lower frequency as the permittivity increases.

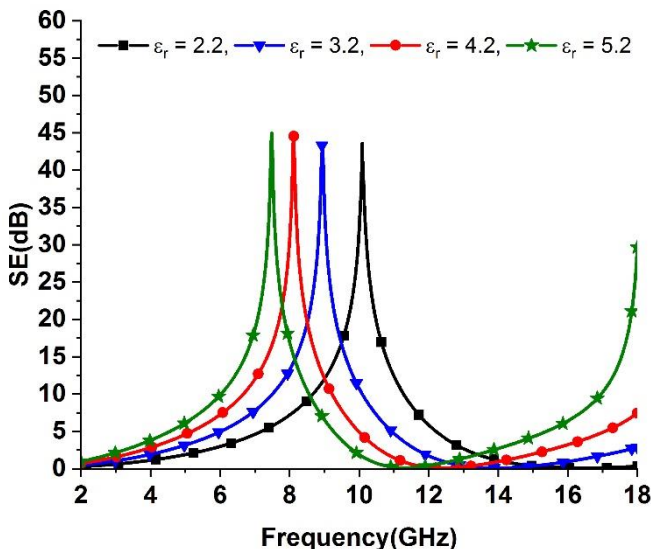


Figure 7: SE of FSS as a function of dielectric constant

IV. CONCLUSION

A novel low-profile FSS shield is presented in this paper. The FSS is designed to suppress communication in the X-band. It provides an attenuation of at least 45 dB centered at 10 GHz frequency. In addition, it offers good angular stability over oblique angle variations. Furthermore, identical, highly selective, angular, and polarization-insensitive responses for TE and TM wave modes are observed, making it a unique EM shield for SATCOM applications in the X-band.

ACKNOWLEDGMENT

This work is supported in part by the National Natural Science Foundation of China (NSFC) under Grants No. 62071306 and 62171289, and in part by Shenzhen Science and Technology Program under Grants JCYJ20200109113601723 and JSGG20210420091805014.

REFERENCES

- [1] B. A. Munk, *Frequency Selective Surfaces: Theory and Design*. John Wiley & Sons, 2000.
- [2] W. -J. Liao, W. -Y. Zhang, Y. -C. Hou, S. -T. Chen, C. Y. Kuo and M. Chou, "An FSS-Integrated Low-RCS Radome Design," *IEEE Antennas and Wireless Propagation Letters*, vol. 18, no. 10, pp. 2076-2080, 2019.
- [3] H. Huang, A. A. Omar and Z. Shen, "Low-RCS and Beam-Steerable Dipole Array Using Absorptive Frequency-Selective Reflection Structures," *IEEE Transactions on Antennas and Propagation*, vol. 68, no. 3, pp. 2457-2462, 2020.
- [4] M. Hosseini and M. Hakkak, "Characteristics Estimation for Jerusalem Cross-Based Artificial Magnetic Conductors," *IEEE Antennas and Wireless Propagation Letters*, vol. 7, pp. 58-61, 2008.
- [5] S. R. Thummalur, R. Kumar and R. K. Chaudhary, "Isolation Enhancement and Radar Cross Section Reduction of MIMO Antenna With Frequency Selective Surface," *IEEE Transactions on Antennas and Propagation*, vol. 66, no. 3, pp. 1595-1600, 2018.
- [6] Muhammad Idrees, Saima Buzdar, Saifullah Khalid, and Muhammad Ali Khalid. "A miniaturized polarization independent frequency selective surface with stepped profile for shielding applications," *Applied Computational Electromagnetics Society Journal*, vol. 31, no. 5, pp. 531-536, 2016.
- [7] G. S. Paul and K. Mandal, "Polarization-Insensitive and Angularly Stable Compact Ultrawide Stop-Band Frequency Selective Surface," *IEEE Antennas and Wireless Propagation Letters*, vol. 18, no. 9, pp. 1917-1921, 2019.
- [8] S. A. B, E. F. Sundarsingh and V. S. Ramalingam, "Mechanically Reconfigurable Frequency Selective Surface for RF Shielding in Indoor Wireless Environment," *IEEE Transactions on Electromagnetic Compatibility*, vol. 62, no. 6, pp. 2643-2646, 2020.
- [9] S. Ünaltd, S. Çimen, G. Çakır and U. E. Ayten, "A Novel Dual-Band Ultrathin FSS With Closely Settled Frequency Response," *IEEE Antennas and Wireless Propagation Letters*, vol. 16, pp. 1381-1384, 2017.
- [10] Bakir, Mehmet, Kemal Delihacioglu, Muharrem Karaaslan, Furkan Dincer, and Cumali Sabah, "U-shaped frequency selective surfaces for single and dual band applications together with absorber and sensor configurations," *IET Microwaves, Antennas & Propagation*, Vol.10, no. 3, pp. 293-300, 2016.
- [11] Z. Zhao, H. Shi, J. Guo, W. Li and A. Zhang, "Stopband Frequency Selective Surface With Ultra-Large Angle of Incidence," *IEEE Antennas and Wireless Propagation Letters*, vol. 16, pp. 553-556, 2017.
- [12] R. Sivasamy, L. Murugasamy, M. Kanagasabai, E. F. Sundarsingh and M. Gulam Nabi Alsath, "A Low-Profile Paper Substrate-Based Dual-Band FSS for GSM Shielding," *IEEE Transactions on Electromagnetic Compatibility*, vol. 58, no. 2, pp. 611-614, 2016.
- [13] Dewani, Aliya A., Steven G. O'Keefe, David V. Thiel, and Amir Galehdar, "Window RF shielding film using printed FSS," *IEEE Transactions on antennas and propagation*, vol. 66, no. 2, pp. 790-796, 2017.